Advances in Nano Research, *Vol. 16, No. 5 (2024) 435-444*
https://doi.org/10.12989/anr.2024.16.5.435

Experimental investigation of mechanical and microstructural properties of concrete containing modified nano-Graphene Oxide

Maryam Ashouri[1a], Ehsanollah Zeighami[*1], Alireza Azarioon[2b], Seyyed Mohammad Mirhosseini[1b] and Sattar Ebrahimi Yonesi[3c]

[1]*Department of Civil Engineering, Arak Branch, Islamic Azad University, Arak, Iran*
[2]*Department of Civil and Architectural Engineering, Malayer University, Malayer, Iran*
[3]*Department of Chemistry, Malayer Branch, Islamic Azad University, Malayer, Iran*

(*Received January 22, 2023, Revised March 30, 2024, Accepted April 1, 2024*)

Abstract. Microscopic defects within the microstructure of hardened cement paste are the main source of weakness in concrete. As a solution, nano-graphene oxide (GO) can be employed to improve the cement paste microstructure. However, there is a number of disadvantages, e.g., fluidity reduction and non-uniform dispersion. The present study sought to modify GO by fabricating a copolymer (PSGO) in a novel process to exploit the advantages of nano-GO while minimizing its disadvantages. Using 0.03wt% copolymerled to 38.8% higher tensile strength, 29.3% higher compressive strength and 25% higher workability. The SEM images revealed that GO and modified GO enhanced concrete by secondary hydration and bonding with C-S-H, creating a firm, integrated, and foil-like structure, and reducing the crack size and depth.
Keywords: compressive strength; copolymer; graphene oxide; scanning electron microscopy; tensile strength

1. Introduction

Improvement of concrete as the most used material in construction industry has been of great interest (Azandariani *et al*. 2022, Berghouti *et al*. 2019). Researchers have sought to introduce methodologies to handle concrete disadvantages, such as low tensile and flexural strengths, vulnerability to environmental agents and brittleness (Ashish and Saini 2018, Hadzima-Nyarko *et al*. 2021, Kim *et al*. 2011). Microscopic defects in the microstructure of hardened cement paste are the main source of weaknesses in concrete, then it is crucial to improve the cement paste microstructure (Akbaş 2018, 2020, Aydogdu *et al*. 2018, Berghouti *et al*. 2019, Moradifard *et al*. 2021, Rodríguez-Pérez *et al*. 2017). Researchers have attempted to partially replace cement as the main substance in concrete production with new alternative materials. This would not only save cement as a strategic product, but also help improve concrete performance by relatively handling its defects. Minerals and organic fibres were initially examined as additives to concrete. Although they somewhat improved the stiffness, durability, and other mechanical properties of concrete, they could not alter the micro-structural nature of cementitious materials (Ebrahimi *et al*. 2019a, Mirjavadi *et al*. 2020a, b, Wang *et al*. 2020). Then, nanomaterials were employed as a solution. Nano-additives significantly enhanced the strength and stiffness of concrete and cope more effectively with microscopic defects (Ebrahimi *et al*. 2019b, Kim *et al*. 2018, Mirjavadi *et al*. 2020c). They effectively improve the cement paste microstructure by influencing the hydration products through secondary hydration and hydration products formation with higher crystalline regularity (Lv *et al*. 2016, Wang *et al*. 2015).

Graphene oxide (GO) is a carbon-based nanomaterial with a monolayer hexagonal structure (Afzali *et al*. 2022, Rodríguez-Pérez *et al*. 2017). It is typically synthesized from graphene using the modified Hummers method (Park and Ruoff 2009). Oxygenfunctionalgroups (typically hydroxyl and epoxide), present on the GO nanosheets, provide covalent bonding to other molecules of materials (Lv *et al*. 2016). GO is also an eco-friendly material, with particles approximately 10^4 times smaller than Portland cement. In contrast to other forms of carbon-based nanomaterials, GO is a hydrophile material and can be conveniently distributed in water (Qiu *et al*. 2010, Sobolev and Ferrada Gutiérrez 2014). GO nanosheetscan undergo strong bonding with the C-S-H phase of Portland cement paste, representing an advantage over other carbon-based nanomaterials, e.g., carbon nanotubes (CNTs) (Gong *et al*. 2015, Lv *et al*. 2013). GO has an elasticity modulus of 23-42 GPa and a tensile strength of nearly 130 MPa, which is much larger than that of cement paste (Dikin *et al*. 2007, Zhu *et al*. 2010). Furthermore, GO can reduce the water absorption of concrete. This is an essential factor, given that permeability plays a key role in the penetration and attack of harmful agents (Wang *et al*. 2015). Microcracks, particularly in the transition zone, are the major explanation for concrete nonlinear behavior and elasticity modulus reduction, specifically at high stress levels. GO nanosheets reduce the thermal cracking potential and more effectively control crack and capillary voids, diminishing crack propagation and enhancing concrete mechanical properties.

*Corresponding author, Associate Professor,
E-mail: eh.zeighami@iau.ac.ir
[a] Ph.D. Student, E-mail: maryam.ashouri@iau.ac.ir
[b] Assistant Professor
[c] Assistant Professor

ISSN: 2287-237X (Print), 2287-2388 (Online)

Devi and Khan (2020) explored the effect of GO on mechanical and durability performance of concrete. They concluded that nanoparticles raised the compressive and tensile strength, and reduced sorptivity and permeability. Chu *et al*. (2020) studied the effect of GO on mechanical properties and durability of ultra-high-performance concrete prepared from recycled sand. It was found that GO enhanced the compressive, flexural and splitting tensile strength, and elastic modulus of concrete. GO also caused a reductionin porosity, increment in resistance of chloride ions penetration, and improvement of freeze–thaw resistance. Lee *et al*. (2020) evaluated the strength of GO-containing cementitious composites. They found optimal GO fraction of 0.025wt% and reported 10.5-41.6% higher compressive strength. Valizadeh Kiamahalleh *et al*. (2020) analysed the mechanical and chemical properties of cementitious composites containing reduced-GO (rGO). They found that 0.1wt% GO led to 53% higher tensile strength and 91% higher compressive strength. Feng *et al*. (2021) combined GO with thermoplastic polyurethane (TPU) into a fibre composite with excellent mechanical properties. They demonstrated that strength and stiffness could be effectively improved by adjusting the TPU-GO mass ratio. Load transfer efficiency rose under the optimized stress distributions, leading to improved strength and stiffness. Chuah *et al*. (2018) have shown that GO is prone to agglomeration in cement paste. This phenomenon is a disadvantage of using GO in concrete. After agglomeration, monolayer sheets are converted into multilayer ones. This prevents the uniform distribution of GO nanoparticles within the concrete and induces a stress concentration in the agglomerated areas, leads to diminishing the mechanical properties of the concrete composite (Chuah *et al*. 2018, Li *et al*. 2017). Methodologies have been recently introduced by researchers to modify GO. Wang *et al*. (2017) exploited the chemical function between polyether amine and GO for the polymer-modification of GO in cement paste specimens. They found that GO modification using polymers enhanced GO fluidity and uniformity, andcaused a rise in the molecular weight of polyether. As a result, the negative impact of GO on fluidity was somewhat neutralized, improving the mechanical and rheological properties of cement paste. Shang *et al*. (2015) explored the influences of GO on rheological properties of cement paste upon the use of GO-encapsulated silica fume (GOSF). Theyfound that GOSF had a larger contribution to the rheological and mechanical properties of cement paste. To improve the dispersion of GO in cement mortar, Li *et al*. (2018) used silica sand for separation of GO nanosheets, leading to an improved GO dispersion within the cement mortar, enhanced mechanical properties, and an improved cement paste microstructure. Apart from advantages in mechanical improvement at small mass fractions, GO has a number of disadvantages (Gong *et al*. 2015, Lee *et al*. 2020, Lv *et al*. 2013, Pan *et al*. 2015):

(1) GO sensibly increases viscosity and reduces fluidity and workability of paste, mortar and concrete (Wang *et al*. 2018). The addition of GO to cement paste results in a flocculated structure with plenty of oxygenfunctional groups due to GO high specific surface area. The agglomerated structure wastes a considerable portion of the mix water, increases internal friction, diminishing the fluidity of the cement paste (Chuah *et al*. 2018, Li *et al*. 2017). Therefore, it is necessary to develop a reliable technique to preserve GO-containing concrete performance and improve GO distribution uniformity to make maximum use of GO advantages.

(2) Although GO can be easily dispersed within aqueous phases, it cannot be easily dispersed in cement paste and concrete. A non-uniform and poor dispersion of GO would negatively impact the performance of the cement paste and concrete (Wang *et al*. 2018). This phenomenon not only reduces the positive effects of GO but may also induce negative effects and weaken the cement paste micro-structure. Since GO modification-especially in concrete mixture- has rarely been studied, this paper introduces a novel polymer-based GO modification technique to further exploit GO advantages in concrete.

The innovative aspect of the present research lies in the development of a novel technique for modifying graphene oxide (GO) to overcome its inherent limitations when incorporated into concrete. Traditional utilization of GO in concrete applications has been hindered by challenges such as reduced fluidity and non-uniform dispersion, which can compromise the overall performance of the concrete mixture. To address these issues, the study introduces a pioneering method for fabricating a copolymer (PSGO) to modify GO. By incorporating this modified GO into concrete mixtures, researchers aimed to capitalize on the benefits of nano-GO while mitigating its drawbacks. Specifically, the copolymer modification process was designed to optimize the dispersion of GO within the concrete matrix, thereby enhancing its effectiveness without compromising the fluidity of the mixture. Experimental results demonstrated the efficacy of the PSGO modification technique, with concrete specimens containing 0.03wt% copolymer exhibiting significant improvements in mechanical and microstructural properties. Notably, the modified concrete showed a remarkable 38.8% increase in tensile strength, a 29.3% increase in compressive strength, and a 25% enhancement in workability compared to conventional concrete formulations. Moreover, scanning electron microscopy (SEM) analysis provided visual evidence of the positive impact of both GO and modified GO on the microstructure of the concrete. The images revealed enhanced secondary hydration and bonding between GO particles and the calcium-silicate-hydrate (C-S-H) phase of the cement paste, resulting in the formation of a more cohesive and resilient concrete matrix. Additionally, the incorporation of GO and modified GO contributed to a reduction in crack size and depth, further enhancing the durability and mechanical properties of the concrete. In summary, the innovative PSGO modification technique represents a significant advancement in the utilization of nano-GO in concrete applications. By effectively addressing the limitations associated with conventional GO incorporation, this approach offers a promising avenue for enhancing the performance and sustainability of concrete structures in the construction industry.

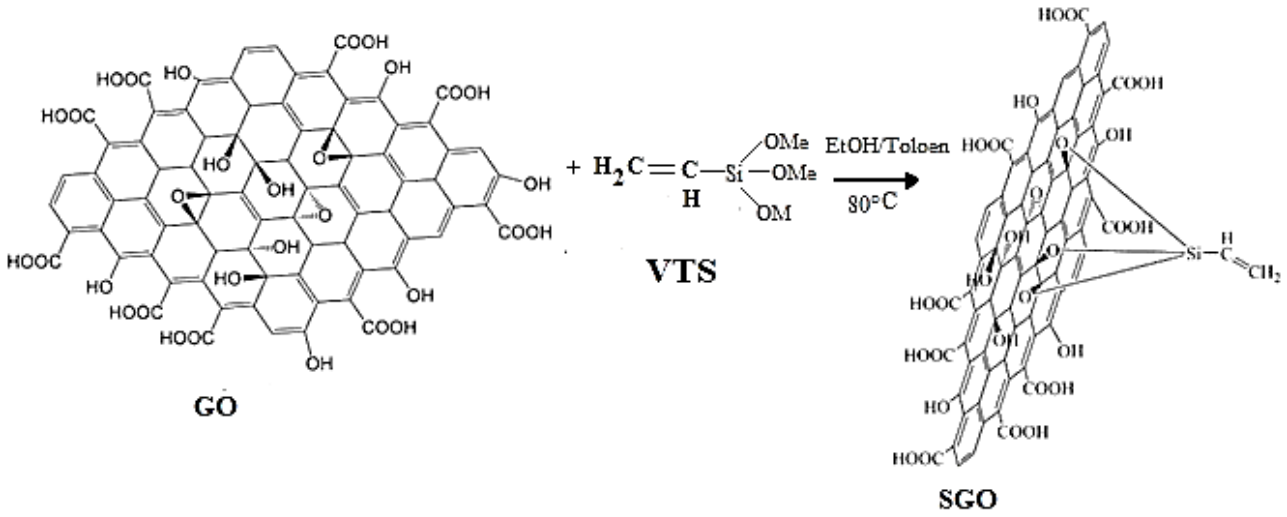

Fig. 1 Synthesis of SGO

The purpose of the research outlined in the text is to address the limitations associated with traditional graphene oxide (GO) utilization in concrete applications by developing a novel modification technique. Traditional GO incorporation in concrete has been hindered by challenges such as reduced fluidity and non-uniform dispersion, which can compromise the overall performance of concrete structures. The primary objective is to capitalize on the benefits of nano-GO while mitigating its drawbacks. Specifically, the copolymer modification process aims to optimize the dispersion of GO within the concrete matrix, thereby enhancing its effectiveness without compromising the fluidity of the mixture. Through experimental investigation, the research aims to demonstrate the efficacy of the PSGO modification technique in improving the mechanical and microstructural properties of concrete. Key parameters such as tensile strength, compressive strength, and workability are evaluated to assess the performance of the modified concrete compared to conventional formulations. Additionally, the study aims to provide visual evidence of the positive impact of both GO and modified GO on the microstructure of concrete through scanning electron microscopy (SEM) analysis. The images are expected to reveal enhanced secondary hydration and bonding between GO particles and the calcium-silicate-hydrate (C-S-H) phase of the cement paste, leading to the formation of a more cohesive and resilient concrete matrix. Furthermore, the incorporation of GO and modified GO is anticipated to contribute to a reduction in crack size and depth, thereby enhancing the durability and mechanical properties of the concrete.

2. Experimental study

All chemicals were purchased from Fluka and Acros Company, and used without further purifications. Ordinary Portland cement (Type I-425) with a compressive strength of 425 kg/cm^2 was employed to fabricate the concrete specimens. Furthermore, manufactured silica sand with a density of 2.46 gr/cm^3, fineness modulus of 3.57 and water absorption of 2.2%, fine gravel with density of 2.6 g/cm^3 and water absorption of 1%, and coarse gravel with a density of 2.68 g/cm^3 and water absorption of 0.8% were used. The aggregates had a maximum size of 19 mm. To obtain sufficient fluidity and workability, PromixUW-154 was employed as a polycarboxylate-based super plasticizer. These materials were mixed using drinking water.

2.1 Synthesis of SGO from GO

50 ml of ethanol/toluene solution (1:1 ratio) and 5 gr of GO was dispersed by an ultrasonic homogenizer (sonicator) for 30 min. Then, vinyltrimethoxysilane (VTS) was added, the mixture was stirringat 80°C for 5 h. The black precipitate was collected from the solution and then washed several times with ethanol. Finally, it was dried at 100°C for 8 h to obtain SGO. Fig. 1 depicts the chemical reactions in the process.

2.2 Synthesis of copolymer from SGO

To preparation of the GO copolymer (PSGO), in first balloon 4 gr of the SGO was added to 30 ml of distilled water and dispersed by ultrasonic vibration for 30 min. After dispersion, a mixture of polyethylene glycol methacrylate (PGM) and ammoniumpersulfate (APS) was added to the mixture in a four-necked flask, and stirred to at 80 °C water bath for 1 h. In second balloon acrylic acid (AA) and 3-mercaptopropionic acid (4.5:0.2 ratio) was added in 5 ml distilled water and stirred. Then a solution of ascorbic acid (2%) was added. Finally the second balloon solutions was added drop wise to the first. After completion of dropping the mixture, it was maintained at this temperature for 2 h. After completion of the reaction, the solution was cooled at room temperature and filtered. The product was washed with distilled water several times and dried at 100 °C for 12 h to obtained copolymer (PSGO). The chemical reactions in the process are shown in Fig. 2.

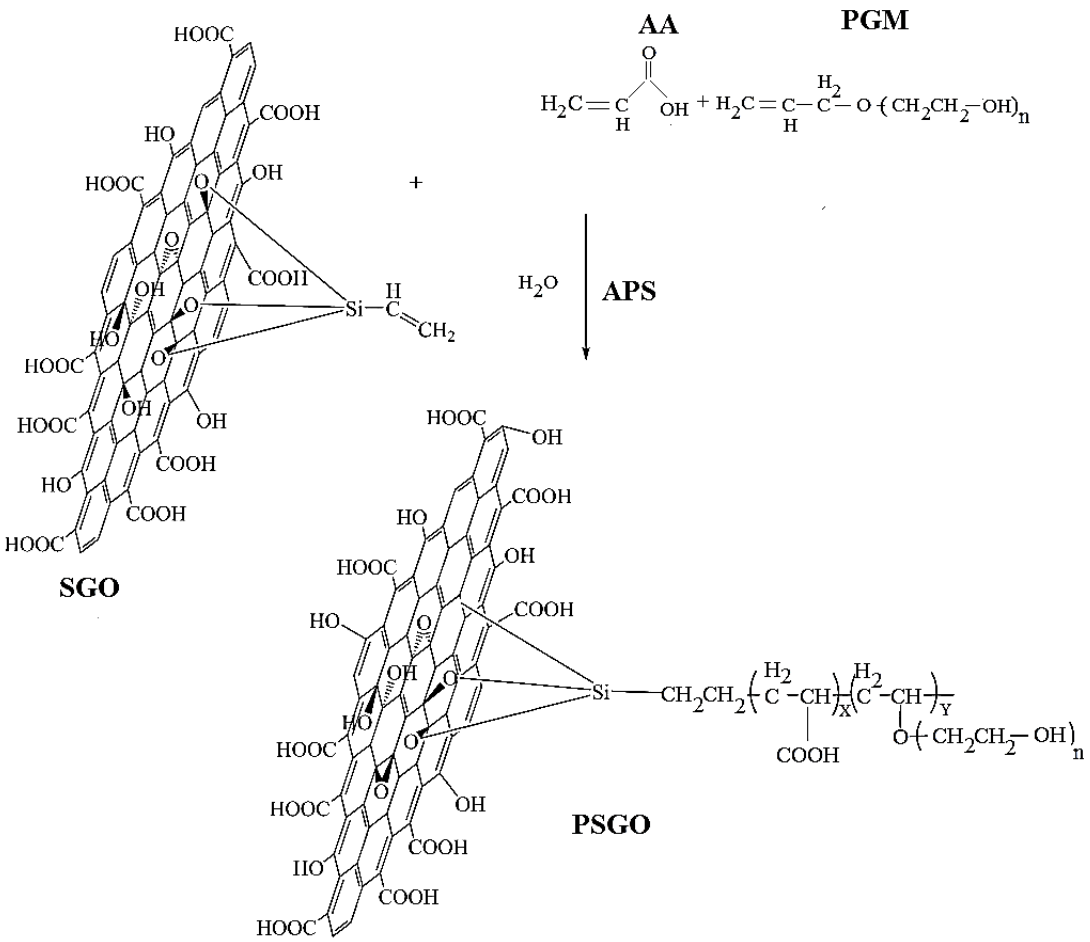

Fig. 2 Synthesis of PSGO (Arnett *et al*. 2007)

Table 1 Physical characteristics of aggregates

Type of aggregate	Specific weight (g/cm^2)	Water absorption %
Fine sand	2.46	2.2
Coarse aggregate	2.68	1.0

2.3 Aggregate

2.3.1 Fine sand

Standard sand produced by Tara Beton Hamadan Company has been used in making concrete specimens. It is of crushed and siliceous type, with a specific gravity of 2.46 grams per cubic centimeter, a modulus of elasticity of 3.57, and a water absorption of 2.2 %.

2.3.2 Coarse aggregate

The gravel used in making the specimens is of local crushed type and obtained from the Pol-e Doab mine, with a maximum size of 19 millimeters for almond gravel and a maximum size of 12 millimeters for chickpea gravel. The density is 2.68 for coarse aggregate. The water absorption for coarse aggregate is 1 % (Table 2).

Tests were performed on the stone materials according to ASTM standards:

(i) Particle size distribution test according to ASTM C131 (1989) and ASTM C535 (2016).

Table 2 The results of the granulation test of stone materials

Sieve number	Sieve size (mm)	The weight percentage of passing materials	
		Sand	Coarse
1	25	100	100
3/4	19	100	75.3
1/2	12.5	100	47.96
3/8	9.5	100	25.17
4	4.75	100	1.42
8	2.36	100	0
16	1.18	69.4	0
30	0.6	44.3	0
50	0.3	16.2	0
100	0.15	6.96	0
200	0.075	0.00	0

(ii) Determination of saturated density with dry surface and sand water absorption capacity according to ASTM C33 (2018).

(iii) Determination of saturated density with dry surface and gravel water absorption capacity according to ASTM C33 (2018).

The physical specifications of the aggregates are presented in Table 1, the results of the aggregate grading in Table 2, and the grading curve in Fig. 3.

Table 3 Mix designs

Mix design	Cement (kg/m^3)	Water (kg/m^3)	Aggregate (kg/m^3)	GO (wt%)	Copolymer (wt%)
C0	350	140	1850	-	-
CG	350	140	1850	0.03	-
CP	350	140	1850	-	0.03

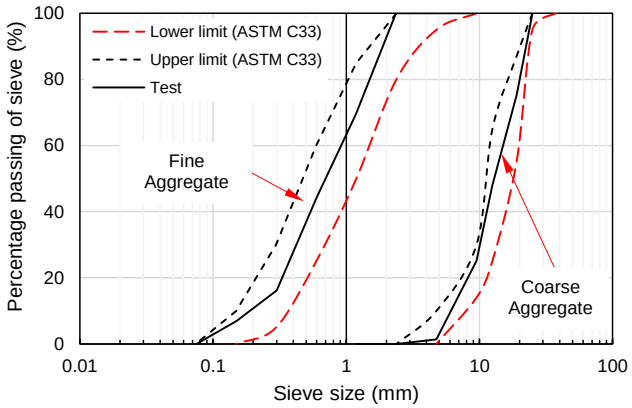

Fig. 3 Granulation curve of stone materials

2.4 Fabrication and maintenance of the specimens

Three mix designs were applied to build three series of specimens, as shown in Table 3. The aggregate mixture consisted of 50% sand, 20% coarse gravel, and 30% fine gravel. The specimens were fabricated and maintained under the same conditions, with 0.03wt% super plasticizer in all series. To more effectively disperse GO and copolymer in the concrete, an ultrasonic homogenizer was used in CG and CP mix designs. GO was mixed with SGO and 500 gr of water and stirred within the homogenizer at 60°C for 30 min. To load electrostatic charges on particles for higher dispersion, 6 gr of the super plasticizer was added to the solution. Fig. 4 depicted the ultrasonic homogenizer instrument.

The mixing procedure of concrete is performed as follows. Once the inner surface of the concrete mixer was wetted, about half of the aggregates with all of the cement were placed within the mixer to be stirred for nearly 2 min. Then, about 70% of the water, the remainder of aggregates, and the super plasticizer, whose optimal fraction was found through the trialmixes, were added. Then the mixing continued for 2-3 min. The solution containing GO or PSGO and the remainder of the water were added to the mixture. After measuring of the slump of fresh concrete, the specimens were moulded. For each series, nine 100 × 100 × 100 mm cubic specimens and nine 100 × 200mm cylindrical specimens were fabricated, as shown in Fig. 5. The specimens were demoulded after 24±2 h and placed in storage pond of water and lime at 23±2°C to be cured.

2.5 Tests of concrete specimens

Workability is the ability of concrete to be mixed, handled, transported and placed with minimum loss of homogeneity, i.e. segregation or bleeding. Workability of the fresh concrete was performed as per ASTM C143. The slump value for different mixes wererecorded for investigating the influence of GO and PSGO in the fluidity of concrete.

Fig. 4 Ultrasonic homogenizer

Fig. 5 Fabricated specimens

Compressive strength tests were performed on cubic samples 7, 28 and 90 days after the samples were mixed for each mix design. A 2000 KN ADR hydraulic press was used for the tests, according to BS1881-116. The splitting tensile strength tests were done according to ASTM C469 on cylindrical samples for each mix design.

X-ray diffraction (XRD) was performed on Unisantis XMD 300 X-Pert (Cu-Ka radiation, λ = 0.15405 nm) over the range 2θ = 20–80° using 0.04 as the step length. The scanning electron microscope measurement (SEM) was carried out on a JSM-840A field emission-scanning electron microscope (FE-SEM).

3. Results and discussion

3.1 Compressive strength

The compressive test was carried out at curing ages of 7, 28, and 90 days. The results are shown in Fig. 6. According

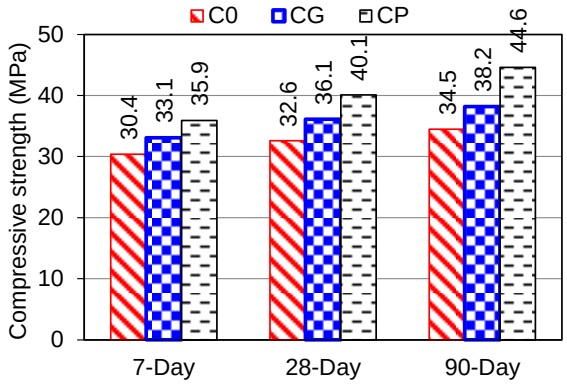

Fig. 6 Compressive strength at different curing ages

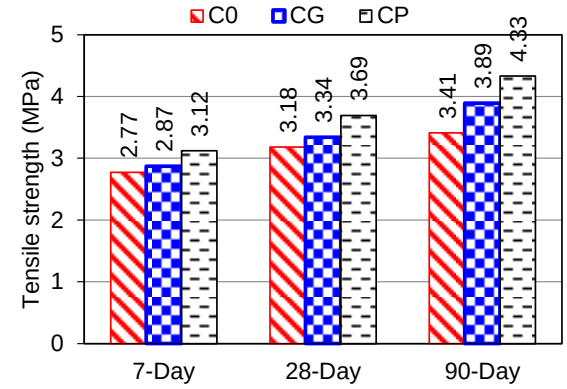

Fig. 7 Splitting tensile strength at different ages

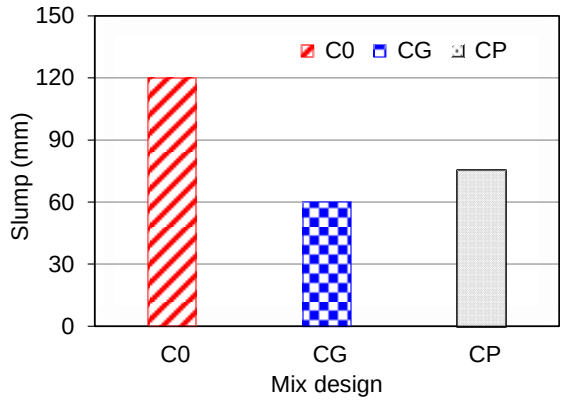

Fig. 8 Concrete workability

to Fig. 6, the compressive strength of CP mix design containing PSGO was higher than that of C0 and CGmix designs. The compressive strengths of CG and CPmix designs were 10.7% and 29.3% higher than that of C0 at the age of 90 days, respectively.

3.2 Tensile strength

Fig. 7 represents the tensile strengths of the specimens at curing ages of 7, 28, and 90 days. According to Fig. 7, CP mix design had higher tensile strength than CG and C0. CG and CP mix designs were found to have 18.4% and 38.8% higher tensile strengths than C0 at the age of 90 days, respectively.

The enhanced mechanical properties of CG and CP mix designs can be attributed to the effects of GO and PSGO on the hydration products through secondary hydration, which effectively improved the cement paste microstructure. It seems thatthe strong bonding of GO and PSGO nanosheets to the C-S-H phase of cement paste and the effective control of capillary voids and cracks by the nanosheets significantly diminished the potential of cracking and enhanced the mechanical properties of concrete. Furthermore, the further increase in the tensile and compressive strengths of CP compared to CG mix design seemingly arose from the modified GO structure and more uniform GO distribution in concrete.

3.3 Slump test

The slump test was performed on fresh concrete. Fig. 8 depicts the workability trend of the concrete samples. According to Fig. 8, CG mix design have a 50% lower workability than C0. This can be attributed to the reduced free water content in the concrete and increased internal friction due to agglomeration. Furthermore, CP mix design showed only 38% lower workability than C0. Hence, the GO modification enhanced concrete workability. This could have arisen from the higher uniformity of PSGO than GO in the concrete.

3.4 XRD

X-ray diffraction (XRD) tests for concrete involve grinding the sample into a fine powder, mounting it onto a sample holder, and analyzing it using a specialized instrument called an X-ray diffractometer. By measuring the diffraction pattern produced when X-rays interact with the crystalline structure of the sample, XRD enables the identification of minerals present in the concrete, including portlandite, ettringite, calcium silicate hydrate (C-S-H), quartz, calcite, and various phases of cement clinker. This qualitative analysis aids in understanding the composition and properties of the concrete, such as its strength, durability, and susceptibility to alkali-silica reaction (ASR) or sulfate attack. Additionally, XRD can provide quantitative information about the relative abundances of different minerals, offering insights into the concrete's performance and informing quality control processes in the construction industry.

3.4.1 XRD spectra of GO, SGO, and PSGO

The XRD spectra of the compounds are illustrated in Fig. 9. As can be seen, three peaks appeared at 2θ=12, 26, and 42° in the spectrum of CGmix design.It should be noted that 2θ denotes the angle between the incident and reflected beams and helps detect minerals in a compound. The peaks remained unchanged in the XRD spectrum of CGmix design. However, the shift in one peak from 2θ=12° to 2θ=19° in the XRD spectrum of CP mix design implies the bonding of the reduction agent to GO, leads to a changing in the layers. Furthermore, the peaks at 2θ=39° explained the fabrication of a copolymer and the bonding of the water reducer to CGmix design. The peak at 2θ=26° corresponds to the graphite layers.

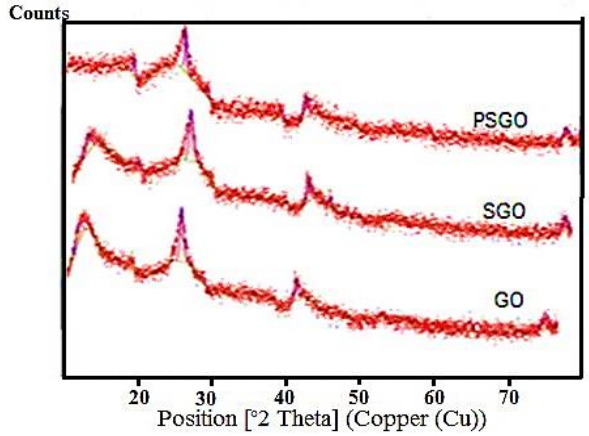

Fig. 9 XRD spectra of GO, SGO, and PSGO

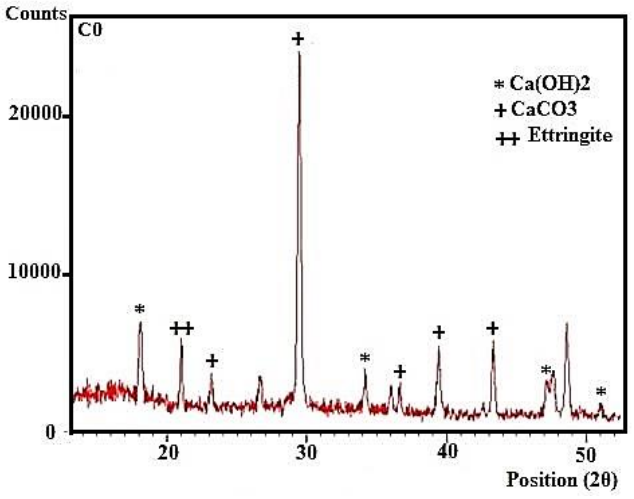

Fig. 10 XRD spectrum of C0 mix design

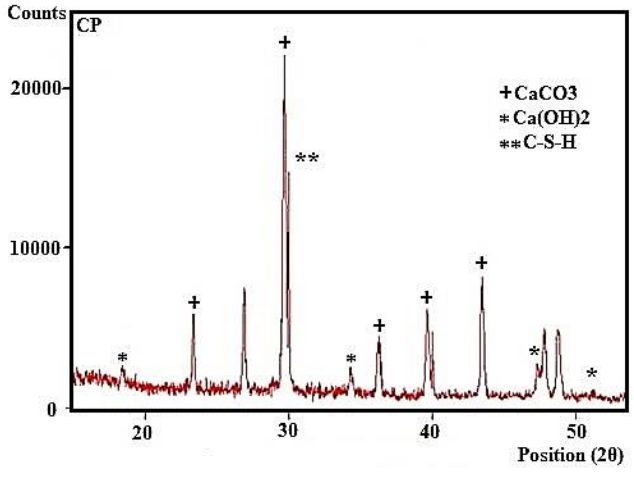

Fig. 11 XRD spectrum of CP mix design

3.4.2 XRD spectra of the mix designs

Fig. 10 depicts the XRD spectrum of C0mix design. The spectrum shows a variety of compounds, e.g., $Ca(OH)_2$ and $CaCO_3$. According to Fig. 10, the peaks in the XRD spectrum of C0 mix design corresponded to $Ca(OH)_2$ at 2θ = 18, 34, 47, and 51°, while those at 2θ=23, 29, 36, 39, and 43° corresponded to $CaCO_3$. The carboxylic acid groups in SGO acidized the composition and changed $Ca(OH)_2$ into $CaCO_3$, as reflected in the XRD spectrum of CGmix design. Fig. 11 shows the XRD spectrum of CP mix design. As can be seen, the intensity of the peaks corresponding to $Ca(OH)_2$ reduced, while that of the peaks corresponding to $CaCO_3$ increased. Table 4 compares the intensities of the peaks corresponding to $CaCO_3$ and $Ca(OH)_2$ in C0 and CP mix designs. As can be seen, CP mix design had a significantly higheramount of $CaCO_3$and significantly lower amount of $Ca(OH)_2$ than C0mix design.

Table 4 Comparison of the peaks corresponding to $CaCO_3$ and $Ca(OH)_2$

$CaCO_3$ Peak (cps)			$Ca(OH)_2$ Peak (cps)		
2θ	C0	CP	2θ	C0	CP
23°	3574	6013	18°	7339	2712
29°	24186	24186	34°	4212	2653
36°	3127	4539	47°	3255	2712
39°	5360	6308	51°	1914	1238
43°	5871	8430	-	-	-

3.5 SEM

Scanning Electron Microscopy (SEM) tests for concrete involve the examination of concrete microstructure at high magnification using a scanning electron microscope. Concrete samples are prepared by cutting, grinding, and polishing to expose the internal structure, followed by coating with a conductive material to prevent charging under the electron beam. SEM analysis provides detailed information about the morphology, distribution, and interfacial characteristics of the various phases within the concrete matrix, including aggregates, cement paste, and any supplementary cementitious materials (SCMs). This information is valuable for understanding factors influencing concrete performance, such as strength, durability, and the effectiveness of admixtures. Additionally, SEM can aid in investigating issues like cracking, alkali-silica reaction (ASR), and other forms of deterioration. Dosage determination for concrete involves optimizing the proportions of cement, aggregates, water, and admixtures to achieve desired properties such as strength, workability, and durability. This process typically involves laboratory testing, mix design calculations, and consideration of factors such as material properties, environmental conditions, and project requirements to determine the most suitable concrete mix proportions. Advanced techniques like SEM can provide insights into the microstructural effects of different dosage combinations, aiding in the refinement of concrete mix designs for optimal performance in specific applications. Dose determination in SEM experiments refers to the process of optimizing the parameters used during imaging to achieve the best possible results for a particular sample. This involves adjusting variables such as the accelerating voltage, probe current, working distance, and magnification to ensure optimal resolution, contrast, and signal-to-noise ratio. The accelerating voltage determines the energy of the electrons

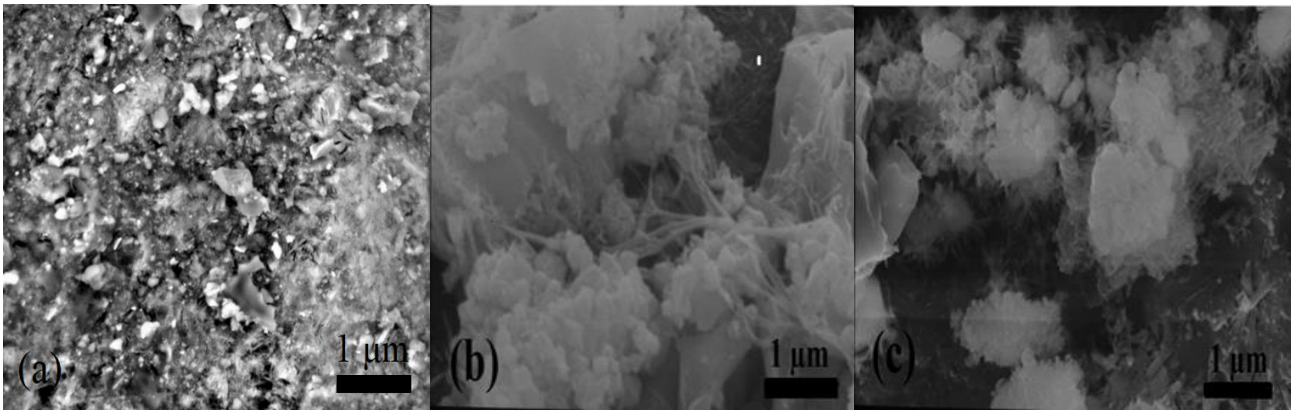

(a) (b) (c)

Fig. 12 SEM image of (a) C0, (b) CG, and (c) CP mix design

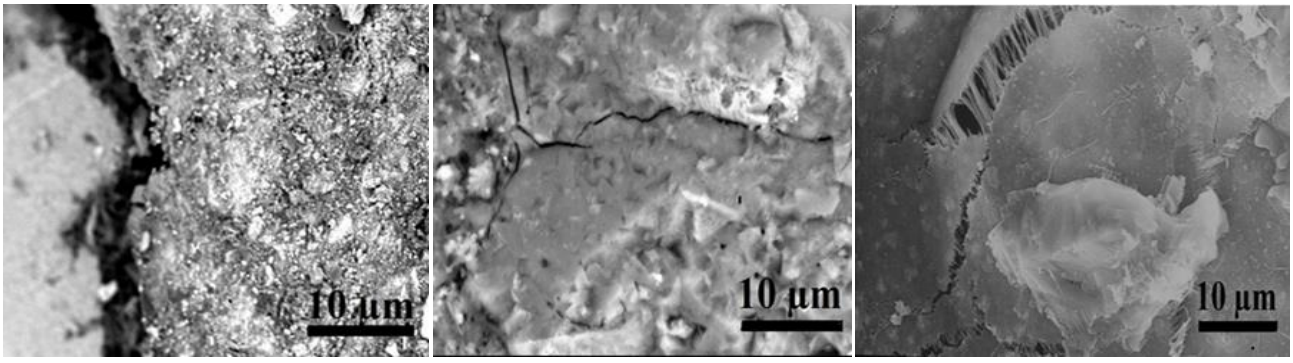

(a) (b) (c)

Fig. 13 SEM image of (a) C0, (b) CG, and (c) CP mix designs in the vicinity of a crack

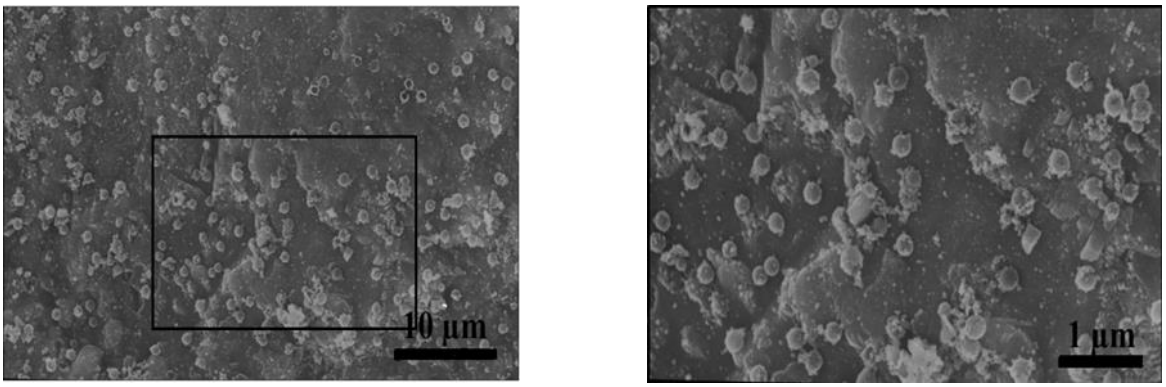

Fig. 14 SEM image of CP mix design on the surface of cement particles

in the electron beam, affecting the depth of penetration into the sample and the interaction volume, while the probe current influences the intensity of the electron beam and thus the signal strength. The working distance refers to the distance between the electron source and the sample surface, which affects both focus and depth of field. Magnification determines the degree of enlargement of the image, influencing the level of detail captured. By carefully optimizing these parameters, dose determination aims to produce high-quality SEM images that provide clear and informative insights into the microstructure and composition of the sample being analyzed. In the present study, the determination of dosage in SEM experiments was conducted meticulously, optimizing parameters such as accelerating voltage, probe current, working distance, and magnification to ensure optimal resolution and contrast. Our approach aimed to achieve the best possible imaging conditions to accurately characterize the microstructure and composition of the concrete samples.

Fig. 12 depicts the SEM images of C0, CG, and CP mix designs at the age of 28 days. The cauliflower-like regions within (b) and (c) represent the C-S-H gel formation in secondary hydration process upon the addition of GO or PSGO. Such spots are not observed in the SEM image of C0 mix design.

Fig. 13 depicts the SEM images of C0, CG, and CP mix

designs in the vicinity of cracks. GO creates a compact, foil-like structure. Wide and deep cracks change into shorter, discrete, shallower and narrower ones. PSGO bridges two sides of some cracks and prevents crack propagation. It seems that the carboxyl (-COOH) and hydroxyl (-OH) groups in the copolymer acidize the concrete environment, convert $Ca(OH)_2$ into $CaCO_3$ and create an adhesive-like structure.

Fig. 14 depicts the SEM image of CP mix design. As can be seen, the cement particle surface was covered with C-S-H after hydration process for 28 days. These C–S–H were numerous and evenly distributed. The C–S–H on the cement surface appears denser and more uniform than that of Portland cement paste.

4. Conclusions

The quantitative and qualitative results was summarized as follows:

(1) CG and CP mix designs had 10.7% and 29.3% higher compressive strength than C0 at the curing age of 90 days, respectively. This indicates that both GO and PSGO enhanced the compressive strength of concrete, however, PSGO applied a 17% improvement in compressive strength in light of polymerization, which is a substantial contribution.

(2) CG and CP mix designs showed 18.4% and 38.8% higher tensile strength than C0 mix design at the age of 90 days, respectively. Hence, it can be concluded that both GO and PSGO enhanced the tensile strength of concrete, however, PSGO had a nearly 17% greater contribution.

(3) A comparison of the tensile and compressive strengths indicted that tensile strength experienced a larger enhancement than compressive strength upon the addition of GO and PSGO. As tensile strength is a drawback of concrete, PSGO may be helpful in handling this drawback. It can be said that PSGO was efficient and effective in enhancing the tensile strength of concrete as an objective of the present study.

(4) The concrete underwent a 50% reduction in workability upon the addition of GO, however, PSGO reduced concrete workability by 38%. This difference may have arisen from the higher distribution uniformity of PSGO than GO within the concrete. Thus, the modification of GO through polymerization could handle the workability reduction challenge to a great extent.

(5) As CP mix design showed larger tensile and compressive strength enhancements than CG mix design, it can be inferred that PSGO had significantly higher uniformity than GO in concrete. A more uniform distribution of particles would lead to a more uniform distribution of stresses, improving the mechanical properties.

(6) An XRD comparison of the control and modified specimens revealed a change in the nanosheets, the carboxylic acid groups of PSGO reduced $Ca(OH)_2$ and increased $CaCO_3$, enhancing concrete tensile and compressive strengths.

(7) A comparison of the SEM images showed that both GO and PSGO created a firm, integrated, and foil-like structure with reduced crack sizes and depths in light of secondary hydration and bonding to the C-S-H phase, leading to enhanced concrete stiffness and likely durability, which was an objective of the present work.

References

Afzali, M., Rostamiyan, Y., Esmaeili, P., Afzali, M., Rostamiyan, Y. and Esmaeili, P. (2022), "Nano-graphene oxide damping behavior in polycarbonate coated on GFRP", *Struct. Eng. Mech.*, Techno-Press, **84**(6), 823. https://doi.org/10.12989/SEM.2022.84.6.823.

Akbaş, Ş.D. (2018), "Forced vibration analysis of cracked functionally graded microbeams", *Adv. Nano Res.*, Techno-Press, **6**(1), 39–55. https://doi.org/10.12989/anr.2018.6.1.039.

Akbaş, Ş.D. (2020), "Modal analysis of viscoelastic nanorods under an axially harmonic load", *Adv. Nano Res.*, **8**(4), 277-282. https://doi.org/10.12989/anr.2020.8.4.277.

Ashish, D.K. and Saini, P. (2018), "Successive recycled coarse aggregate effect on mechanical behavior and microstructural characteristics of concrete", *Comput. Concr.*, **21**(1), 39-46. https://doi.org/10.12989/cac.2018.21.1.039.

ASTM Standard Test (2018), *Standard Specification for Concrete Aggregates, American Society for Testing Materials*, ASTM-C33.

ASTM Standard Test (2016), *Standard Test Method for Resistance to Degradation of Large-Size Coarse Aggregate by Abrasion and Impact in the Los Angeles Machine*, ASTM-C535, Philadelphia.

ASTM Standard Test, (1989), *Standard Test Method for Resistance to Degradation of Small-Size Coarse Aggregate by Abrasion and Impact in the Los Angeles Machine*, ASTM C131, Philadelphia.

Aydogdu, M., Arda, M. and Filiz, S. (2018), "Vibration of axially functionally graded nano rods and beams with a variable nonlocal parameter", *Adv. Nano Res.*, **6**(3), 257-278. https://doi.org/10.12989/anr.2018.6.3.257.

Azandariani, M. G., Gholami, M. and Nikzad, A. (2022), "Eringen's nonlocal theory for non-linear bending analysis of BGF Timoshenko nanobeams", *Adv. Nano Res.*, **12**(1), 37. https://doi.org/10.12989/ANR.2022.12.1.037.

Berghouti, H., Bedia, E.A.A., Benkhedda, A. and Tounsi, A. (2019), "Vibration analysis of nonlocal porous nanobeams made of functionally graded material", *Adv. Nano Res.*, **7**(5), 351-364. https://doi.org/10.12989/anr.2019.7.5.351.

Chu, H., Zhang, Y., Wang, F., Feng, T., Wang, L. and Wang, D. (2020), "Effect of graphene oxide on mechanical properties and durability of ultra-high-performance concrete prepared from recycled sand", *Nanomaterials*, MDPI AG, **10**(9), 1718. https://doi.org/10.3390/nano10091718.

Chuah, S., Li, W., Chen, S. J., Sanjayan, J. G. and Duan, W. H. (2018), "Investigation on dispersion of graphene oxide in cement composite using different surfactant treatments", *Constr. Build. Mater.*, Elsevier Ltd, **161**, 519-527. https://doi.org/10.1016/j.conbuildmat.2017.11.154.

Devi, S.C. and Khan, R.A. (2020), "Effect of graphene oxide on mechanical and durability performance of concrete", *J. Build. Eng.*, **27**, 101007. https://doi.org/10.1016/j.jobe.2019.101007.

Dikin, D.A., Stankovich, S., Zimney, E.J., Piner, R.D., Dommett, G.H.B., Evmenenko, G., Nguyen, S.T. and Ruoff, R.S. (2007), "Preparation and characterization of graphene oxide paper", *Nature*, **448**(7152), 457-460. https://doi.org/10.1038/nature06016.

Ebrahimi, F., Nouraei, M., Dabbagh, A. and Civalek, Ö. (2019a), "Buckling analysis of graphene oxide powder-reinforced nano-composite beams subjected to non-uniform magnetic field",

Struct. Eng. Mech., **71**(4), 351-361. https://doi.org/10.12989/sem.2019.71.4.351.

Ebrahimi, F., Nouraei, M., Dabbagh, A. and Rabczuk, T. (2019b), "Thermal buckling analysis of embedded graphene-oxide powder-reinforced nanocomposite plates", *Adv. Nano Res.*, **7**(5), 293-310. https://doi.org/10.12989/anr.2019.7.5.293.

Feng, L., Li, Y., Luan, Y., Guo, Z., Xu, F. and Zhang, X. (2021), "Bioinspired nacre-like GO-based fiber with improved strength and toughness by staggered layer structure regulation and interface modification", *Mech. Adv. Mater. Struct.*, **29**(26), 5215-5224. https://doi.org/10.1080/15376494.2021.1950876.

Gong, K., Pan, Z., Korayem, A.H., Qiu, L., Li, D., Collins, F., Wang, C.M. and Duan, W.H. (2015), "Reinforcing effects of graphene oxide on portland cement paste", *J. Mater. Civ. Eng., ASCE*, **27**(2), A4014010. https://doi.org/10.1061/(asce)mt.1943-5533.0001125.

Hadzima-Nyarko, M., Nyarko, K.E., Djikanovic, D. and Brankovic, G. (2021), "Microstructural and mechanical characteristics of self-compacting concrete with waste rubber", *Struct. Eng. Mech.*, **78**(2), 175-186. https://doi.org/10.12989/sem.2021.78.2.175.

Kim, B., Taylor, L., Troy, A., McArthur, M. and Ptaszynska, M. (2018), "The effects of Graphene Oxide flakes on the mechanical properties of cement mortar", *Comput. Concr.*, **21**(3), 261-267. https://doi.org/10.12989/cac.2018.21.3.261.

Kim, J.J., Fan, T. and Reda Taha, M.M. (2011), "A homogenization approach for uncertainty quantification of deflection in reinforced concrete beams considering micro-structural variability", *Struct. Eng. Mech.*, **38**(4), 503-516. https://doi.org/10.12989/sem.2011.38.4.503.

Lee, S.J., Jeong, S.H., Kim, D.U. and Won, J.P. (2020), "Graphene oxide as an additive to enhance the strength of cementitious composites", *Compos. Struct.*, **242**, 112154. https://doi.org/10.1016/j.compstruct.2020.112154.

Li, X., Li, C., Liu, Y., Chen, S.J., Wang, C.M., Sanjayan, J.G. and Duan, W. H. (2018), "Improvement of mechanical properties by incorporating graphene oxide into cement mortar", *Mech. Adv. Mater. Struct.*, **25**(15-16), 1313-1322. https://doi.org/10.1080/15376494.2016.1218226.

Li, X., Liu, Y.M., Li, W.G., Li, C.Y., Sanjayan, J.G., Duan, W.H. and Li, Z. (2017), "Effects of graphene oxide agglomerates on workability, hydration, microstructure and compressive strength of cement paste", *Constr. Build. Mater.*, **145**, 402-410. https://doi.org/10.1016/j.conbuildmat.2017.04.058.

Lv, S.H., Deng, L.J., Yang, W.Q., Zhou, Q.F. and Cui, Y.Y. (2016), "Fabrication of polycarboxylate/graphene oxide nanosheet composites by copolymerization for reinforcing and toughening cement composites", *Cem. Concr. Compos.*, **66**, 1-9. https://doi.org/10.1016/j.cemconcomp.2015.11.007.

Lv, S., Ma, Y., Qiu, C., Sun, T., Liu, J. and Zhou, Q. (2013), "Effect of graphene oxide nanosheets of microstructure and mechanical properties of cement composites", *Constr. Build. Mater.*, **49**, 121-127. https://doi.org/10.1016/j.conbuildmat.2013.08.022.

Mirjavadi, S. S., Forsat, M., Barati, M. R. and Hamouda, A. M. S. (2020a), "Assessment of transient vibrations of graphene oxide reinforced plates under pulse loads using finite strip method", *Comput. Concr.*, **25**(6), 575-585. https://doi.org/10.12989/cac.2020.25.6.575.

Mirjavadi, S.S., Forsat, M., Barati, M.R. and Hamouda, A.M.S. (2020b), "Post-buckling analysis of geometrically imperfect tapered curved micro-panels made of graphene oxide powder reinforced composite", *Steel Compos. Struct.*, **36**(1), 63-74. https://doi.org/10.12989/scs.2020.36.1.063.

Mirjavadi, S.S., Forsat, M., Yahya, Y.Z., Barati, M.R., Jayasimha, A.N. and Khan, I. (2020c), "Finite element based post-buckling analysis of refined graphene oxide reinforced concrete beams with geometrical imperfection", *Comput. Concr.*, **25**(4), 283-291. https://doi.org/10.12989/cac.2020.25.4.283.

Moradifard, R., Gholami, M. and Zare, E. (2021), "Nonlinear free vibration analysis of a bi-directional functionally graded microbeam on nonlinear elastic foundation using modified couple stress theory", *Int. J. Comput. Mater. Sci. Eng.*, **10**(1). https://doi.org/10.1142/S2047684121500019.

Pan, Z., He, L., Qiu, L., Korayem, A.H., Li, G., Zhu, J.W., Collins, F., Li, D., Duan, W. H. and Wang, M.C. (2015), "Mechanical properties and microstructure of a graphene oxide-cement composite", *Cem. Concr. Compos.*, **58**, 140-147. https://doi.org/10.1016/j.cemconcomp.2015.02.001.

Park, S. and Ruoff, R.S. (2009), "Chemical methods for the production of graphenes", *Nat. Nanotechnol.*, **4**(4), 217-224. https://doi.org/10.1038/nnano.2009.58.

Qiu, L., Yang, X., Gou, X., Yang, W., Ma, Z.F., Wallace, G.G. and Li, D. (2010), "Dispersing carbon nanotubes with graphene oxide in water and synergistic effects between graphene derivatives", *Chem. A Eur. J.*, 10653-10658. https://doi.org/10.1002/chem.201001771.

Rodríguez-Pérez, M., Villanueva-Cab, J. and Pal, U. (2017), "Evaluation of thermally and chemically reduced graphene oxide films as counter electrodes on dye-sensitized solar cells", *Adv. Nano Res.*, **5**(3), 231-244. https://doi.org/10.12989/anr.2017.5.3.231.

Shang, Y., Zhang, D., Yang, C., Liu, Y. and Liu, Y. (2015), "Effect of graphene oxide on the rheological properties of cement pastes", *Constr. Build. Mater.*, **96**, 20-28. https://doi.org/10.1016/j.conbuildmat.2015.07.181.

Sobolev, K. and Ferrada Gutiérrez, M. (2014), "How nanotechnology can change the concrete world", *Prog. Nanotechnol.*, 113-116. https://doi.org/10.1002/9780470588260.ch16.

Valizadeh Kiamahalleh, M., Gholampour, A., Tran, D.N.H., Ozbakkaloglu, T. and Losic, D. (2020), "Physiochemical and mechanical properties of reduced graphene oxide-cement mortar composites: Effect of reduced graphene oxide particle size", *Constr. Build. Mater.*, **250**, 118832. https://doi.org/10.1016/j.conbuildmat.2020.118832.

Wang, Q., Cui, X., Wang, J., Li, S., Lv, C. and Dong, Y. (2017), "Effect of fly ash on rheological properties of graphene oxide cement paste", *Constr. Build. Mater.*, Elsevier Ltd, **138**, 35-44. https://doi.org/10.1016/j.conbuildmat.2017.01.126.

Wang, Q., Li, S. Y., Pan, S. and Guo, Z.W. (2018), "Synthesis and properties of a silane and copolymer-modified graphene oxide for use as a water-reducing agent in cement pastes", *New Carbon Mater.*, **33**(2), 131-139. https://doi.org/10.1016/S1872-5805(18)60330-0.

Wang, Q., Wang, J., Lu, C.X., Liu, B. W., Zhang, K. and Li, C.Z. (2015), "Influence of graphene oxide additions on the micro-structure and mechanical strength of cement", *Xinxing Tan Cailiao/New Carbon Mater.*, **30**(4), 349-356. https://doi.org/10.1016/s1872-5805(15)60194-9.

Wang, Y., Xie, K. and Fu, T. (2020), "Size-dependent dynamic stability of a FG polymer microbeam reinforced by graphene oxides", *Struct. Eng. Mech.*, **73**(6), 685-698. https://doi.org/10.12989/sem.2020.73.6.685.

Zhu, Y., Murali, S., Cai, W., Li, X., Suk, J. W., Potts, J.R. and Ruoff, R.S. (2010), "Graphene and Graphene Oxide: Synthesis, Properties, and Applications", *Adv. Mater*, **22**(35), 3906-3924. https://doi.org/10.1002/adma.201001068.

CC